

Annealing behavior of hydrogen traps in Ne-implanted Ta

J. Keinonen, V. Karttunen, J. Räisänen, F.-J. Bergmeister, A. Luukkainen, and P. Tikkanen
Accelerator Laboratory, University of Helsinki, Hämeentie 100, SF-00550 Helsinki, Finland

(Received 9 September 1986)

Annealing behavior of defects attributed to the high-atomic-density neon precipitates in tantalum produced by 4.0×10^{20} – 9.4×10^{21} 60-keV $(^{22}\text{Ne}^+ \text{ ions})/\text{m}^2$ has been studied in the temperature range 300–970 K by ion-beam techniques. Four different recovery stages were observed. Two of these are associated with the Ne-precipitate–Ta-matrix interface affected by the Ne-implantation-induced damage; the recovery energies are 1.8 and 2.1 eV. Stages attributed to the dissociation of Ne_nV_m complexes (2.6 eV) and to stronger Ne_nV_m complexes (> 2.9 eV) are also identified.

Trapping of the hydrogen isotope deuterium in a variety of vacancy structures in different inert-gas-implanted metals has been extensively studied during recent years.^{1–16} Ion-implanted gases heavier than helium have very recently been reported to form precipitates with anomalously high atomic density and solid crystallites which have an epitaxial relation with the host lattice.^{16–23} The trapping of deuterium in such samples can be due to the strain fields surrounding the precipitates, at the precipitate-matrix interface or in the lattice structure of the precipitate particle itself.¹⁶ In order to study hydrogen traps in inert-gas-implanted metals an approach different from the deuterium trapping studies was adopted in the present work.

The aim of this work was to study the annealing behavior of the defects which trap hydrogen in 60-keV Ne-ion-implanted Ta. Changes in the defects were observed indirectly by measuring H concentration profiles at room temperature. Because of the very fast diffusion²⁴ (the preexponential factor $D_0 = 4.4 \times 10^{-4}$ cm²/s, the activation energy $Q = 0.14$ eV) H decorates the remaining traps in Ta immediately after each annealing. Note that due to the experimental procedure the traps observed have H dissociation energies above about 0.9 eV (measurements at room temperature) and no information on energies at higher temperatures was observed. However, based on the information²⁵ on the energies of H at chemisorption, the trap dissociation energies are below about 1.2 eV.

The room-temperature implantation of the 4.0×10^{20} – 9.4×10^{21} 60-keV $(^{22}\text{Ne}^+ \text{ ions})/\text{m}^2$ into Ta and the characterization of the Ne precipitates (the diameters from 15 to 48 Å and atomic Ne densities $n_{\text{Ne}} = 0.095$ – 0.066 Å⁻³, respectively) have been reported in our previous study.²³ The hydrogen was introduced into the Ne-implanted samples by annealing them in atmosphere at room temperature.

Depth profiling of H by the nuclear-resonance-broadening (NRB) technique was carried out at the laboratory tandem accelerator using a $^{15}\text{N}^{2+}$ beam in conjunction with the 6.385-MeV resonance in the $^1\text{H}(^{15}\text{N}, \alpha\gamma)^{12}\text{C}$ reaction.²⁶ The use of the sharp ($\Gamma = 1.8$ keV)^{27,28} resonance made it possible to profile the H distribution with a good depth resolution (about 3 nm at the surface). The depth profiles of H and thus also those of H traps are illus-

trated in Fig. 1. The concentration distribution of Ne, also illustrated in Fig. 1, was measured by the NRB method through the reaction $^{22}\text{Ne}(p, \gamma)^{23}\text{Na}$ at $E_p = 1005$ keV.²⁹ The profiles were measured at least twice to make sure that the probing ^{15}N and proton beams had negligible effects on the H trapping. Atomic Ne densities within the Ne precipitates were studied by means of the Doppler-shift attenuation method.²³

The 1800-s isochronal annealings of the samples were carried out in a quartz-tube furnace in a low-pressure (< 50 μPa), dry argon atmosphere.³⁰ The evolution of the H and Ne concentration profiles were studied in the temperature range 300–970 K. The energies of H at chemisorption²⁵ indicate that above about 450 K, H is released from the traps. Thus, the migration of H traps was studied by measuring the H profiles at room temperature. The

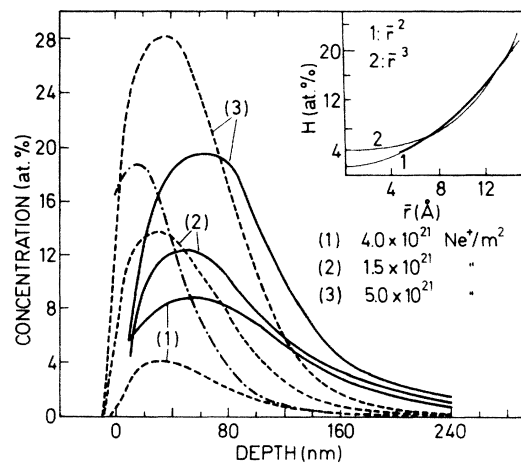


FIG. 1. The experimental concentration distributions of the 60-keV $^{22}\text{Ne}^+$ ions in Ta for different fluences (dashed lines), the experimental H concentration distributions for the corresponding samples (solid lines), and the Monte Carlo simulated damage profile due to the Ne implantation (dot-dashed line). The inset illustrates the dependence of the H concentration on the mean radius of the Ne precipitates. The thin lines are the fitted curves and the thick line represents the experimental data obtained for all the samples at every depth between 80 and 200 nm.

Ne profiles and atomic Ne densities were also measured at room temperature after each annealing.

All the unannealed samples show that the H trap concentrations follow the Ne concentration distributions rather than the Ne implantation-induced damage distribution. The damage distribution shown in Fig. 1, was obtained in a Monte Carlo simulation³¹ which reproduced the experimental range profile of the 60-keV $^{22}\text{Ne}^+$ ions. In the Ne-implantation-induced damage region (0 to about 80 nm), the ratio of the H concentration to the Ne concentration is observed to decrease with increasing Ne fluence and with the Ne-implantation-induced damage. Deeper in the sample (80–200 nm), the amount of trapped H is proportional to the calculated surface area of the Ne precipitates (see inset in Fig. 1). Beyond the Ne profile, the concentration of the untrapped H was less than 0.2 at. %.

The recovery stages of the H traps are illustrated in Fig. 2. The present detailed depth profile analysis shows that there are four different stages starting at temperatures 570, 720, 870, and above 970 K.

At 570 K, a rapid loss of H traps starts in the region where the Ne-implantation-produced damage profile overlaps with the Ne distribution.

At 720 K, H traps start to anneal out from the region where the amount of trapped H is proportional to the calculated surface area of the Ne precipitates.

At 870 K, H traps migrate from the whole area of the Ne concentration profile. The simultaneous migration of Ne is observed. The loss of Ne was observed to be proportional to the fluence and to range from about 8% to 20% for the fluences $\Phi = 4.0 \times 10^{20} - 9.4 \times 10^{21}$ ($^{22}\text{Ne}^+$ ions)/ m^2 , respectively. After this phase the H concentration is constant up to 970 K and about 1 at. %.

It has been shown by different authors¹⁻¹⁶ that in inert gas implantations of metals a large variety of H traps with a broad range of H binding enthalpies (0.24–0.83 eV) are produced. As a possibility for deuterium traps in Ar- and Kr-implanted Ni Frank, McManus, Rehn, and Baldo¹⁶ have suggested the free volume at the interface of the host lattice and the solid Ar and Kr precipitate. Our observation on the surface-area dependence of the trapped H supports this conclusion. The systematic studies^{22,32} on the implanted Ne in different metals indicate that Ne precipi-

tates are solid in Ta. Because of the room-temperature measurements, H traps studied in the present work bind H with enthalpies over 0.7 eV. The energy of 1.3 eV (480 K) has recently been reported³³ for the dissociation of HV complexes in Ta followed by the H and V migration [activation energies for migration 0.14 (Ref. 24) and 0.7 eV (Ref. 33), respectively]. Such a trapping mechanism was not observed in the present work. The simultaneous migration of Ne and H traps at 870 K is in agreement with the obvious formation of Ne_nV_m complexes during the Ne implantation.^{34,35}

The first two stages where no Ne migration was observed are due to the migration of H traps from the interface of the Ta matrix and Ne precipitates. The first stage represents the interface which is strongly affected by the Ne-implantation-induced damage (trapping of vacancies) and the second stage, the interface not significantly affected by the damage. The strong reduction of H traps after the first two stages and the fact that no significant change was observed in the atomic Ne density indicate that the damage at the interface does not have a significant effect on the precipitates. The improvement observed by Evans and Mazey^{20,21} in the Kr diffraction reflections after annealings of Kr-implanted Mo and Ti, is probably due to the loss of defects from the interface. At the third stage H traps migrate from the whole area of the Ne concentration profile. The simultaneous migration of Ne indicates that H was trapped in small Ne_nV_m complexes. The small increase (about 5%) of the atomic Ne density supports the fact that Ne was not migrated from the Ne precipitates. An explanation to the ratio 2:1 of the Ne loss to the H loss could be the dissociation of the Ne_2VH complexes. The low and constant H concentration after the 970-K annealing is probably due to the H traps associated to Ne_nV_m complexes (stronger than those at the third stage) rather than the well-annealed Ta-matrix-Ne-precipitate interface.

The first two recovery stages of H traps were simulated by the following simple model based on Monte Carlo calculations. The changes in the ability of defects to bind H were assumed to be due to the dissociation of vacancies from defects. The migration and trapping of vacancies was described analogously to models used for the migra-

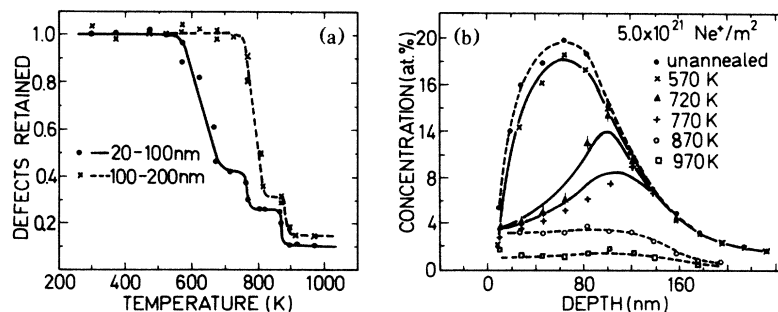


FIG. 2. The annealing behavior of H traps. (a) The recovery curves of H traps in the regions 20–100 nm (solid line) and 100–200 nm (dashed line) are shown separately. Data points are from all the samples studied. The reason behind the fact that at the first stage the curve is not as steep as at the second one is the overlap of the second-stage defects, indicated also by the step in the curve. The third stage can be seen in both curves. (b) The dashed lines are drawn to guide the eye. The solid lines represent the Monte Carlo simulation of the observed annealing behavior.

tion and trapping of atoms.^{31,36,37} The desorption rate of vacancies which disappear in the sinks (the surface of the sample and bulk) is in the first order

$$dn_i/dt = -vn_i, \quad (1)$$

where $n_i(t)$ ($i=1,2$) is the number of vacancies present at time t and v is the rate constant of the vacancies which are assumed to migrate by single jumps using the lattice sites of Ta. Recombination with interstitials was ignored. If the initial number of vacancies in the defects located in the interface of the Ta matrix and Ne precipitate is n_{0i} , the number of vacancies remaining after the anneal of t_a seconds is

$$n_i = n_{0i} \exp[-v_0 t_a \exp(-E_i/k_B T)], \quad (2)$$

where E_i is the activation energy of the dissociation of the vacancies from defects and the frequency factor v_0 is assumed to be 10^{13} s^{-1} . In the case of He_nV complexes in Mo the frequency factor has been reported³⁵ to vary from 10^{13} s^{-1} to 10^{15} s^{-1} . The use of the latter value would increase the deduced recovery energies by 10%.

The distribution of the defects associated with the trapping of Ne-implantation-induced vacancies at the Ta-matrix-Ne-precipitate interfaces was approximated by the overlap of the calculated damage profile and the measured as-implanted H profile. The damage profile was varied according to the Ne fluence. The distribution of the defects not affected by the trapped vacancies was assumed to be the difference between the original H concentration distribution and the H profile observed after the 870-K annealing. Defect distributions are illustrated in Fig. 3.

The trapping time t_i of an individual vacancy in a defect was obtained from Eq. (2) by using a random number R ($0 < R < 1$),

$$t_i = -[\ln(R)/v_0] \exp(E_i/k_B T). \quad (3)$$

Retrapping of vacancies in the defects was assumed to occur if

$$R > [1 - 0.7217C(z,t)]^j, \quad (4)$$

where R is a random number and j ($=30$) the number of jumps. The factor 0.7217 describes the probability of finding a fresh site at each jump.^{36,37} Because the precipitates are not mobile the concentration of the vacancy traps was described by

$$C(z,t) = [c(z,t=0) - c(z,t)]/c(z,t=0), \quad (5)$$

where $c(z,t)$ is the total vacancy concentration in defects at depth z at time t .

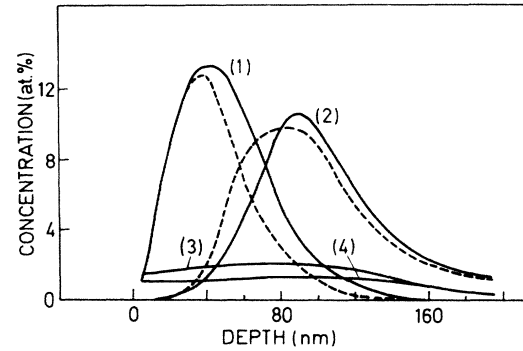


FIG. 3. The H trap distributions used in the Monte Carlo simulation of the annealing behavior of the $\Phi = 5.0 \times 10^{21} \text{ Ne}^+/\text{m}^2$ sample (solid lines) and in that of the $\Phi = 3.0 \times 10^{21} \text{ Ne}^+/\text{m}^2$ sample (dashed lines). The numbers given refer to the four different recovery stages observed.

The distance z after j jumps was³¹

$$\int_{-\infty}^z W(z,j) dz = R, \quad (6)$$

where R is a random number. $W(z,j)$ is the solution of Fick's equation

$$W(z,j) = [1/(2\pi ja^2)^{1/2}] \exp(-z^2/2ja^2), \quad (7)$$

where a is the length of a single jump given by the lattice constant.

Results of the simulation are illustrated in Fig. 2 together with experimental data. It can be seen that the simulation describes well the annealing behavior of the defects. In obtaining the recovery energies $E_1 = 1.8 \text{ eV}$ (570 K) and $E_2 = 2.1 \text{ eV}$ (720 K), the fitting values were the energies and the ratio of the amounts of type-1 and -2 defects.

The distribution of the Ne_nV_m complexes was obtained from the difference between the 870- and 970-K annealing profiles of H. The recovery temperature was about 870 K. From the step in the recovery curve we derived for the recovery energy the value of 2.6 eV with $v_0 = 10^{13} \text{ s}^{-1}$. The use of $v_0 = 10^{15} \text{ s}^{-1}$ would increase the value by 10%.

The defects remaining after the 970-K annealing indicate a recovery energy over 2.9 eV.

In conclusion, the present work on the annealing behavior of H traps located at the interface of the Ta matrix and Ne precipitates gives new information on the recovery stages of inert gas-implantation-induced defects in metals and their strong dependence on the implantation induced damage.

This work has been supported by the Academy of Finland.

¹S. T. Picraux, J. Böttiger, and N. Rud, J. Nucl. Mater. **63**, 110 (1976).

²S. M. Myers, S. T. Picraux, and R. E. Stoltz, Appl. Phys. Lett. **37**, 168 (1980).

³F. Besenbacher, J. Böttiger, T. Laursen, and W. Moller, J. Nucl. Mater. **93-94**, 617 (1980).

⁴S. M. Myers, F. Besenbacher, and J. Böttiger, Appl. Phys. Lett. **39**, 450 (1981).

⁵F. Besenbacher, S. M. Myers, and J. K. Nørskov, Nucl. Instrum. Methods Phys. Res. Sect. B **7/8**, 55 (1985).

⁶S. M. Myers, D. M. Follstaedt, F. Besenbacher, and J. Böttiger, J. Appl. Phys. **53**, 8734 (1982).

- ⁷F. Besenbacher, J. Böttiger, and S. M. Myers, *J. Appl. Phys.* **53**, 3536 (1982).
- ⁸F. Besenbacher and J. Böttiger, *J. Appl. Phys.* **53**, 3547 (1982).
- ⁹F. Besenbacher, B. Beck, B. B. Nielsen, and S. M. Myers, *J. Appl. Phys.* **56**, 3384 (1984).
- ¹⁰M. S. Daw, C. L. Bisson, and W. D. Wilson, *Metall. Trans. A* **14**, 1257 (1983).
- ¹¹J. K. Nørskov, F. Besenbacher, J. Böttiger, B. B. Nielsen, and A. A. Pisarev, *Phys. Rev. Lett.* **49**, 1420 (1982).
- ¹²S. M. Myers, W. R. Wampler, F. Besenbacher, S. L. Robinson, and N. R. Moody, *Mater. Sci. Eng.* **69**, 397 (1985).
- ¹³F. Besenbacher, S. M. Myers, and J. K. Nørskov, *Nucl. Instrum. Methods Phys. Res. Sect. B* **7/8**, 55 (1985).
- ¹⁴P. Borgesen, B. M. U. Scherzer, and W. Moller, *J. Appl. Phys.* **57**, 2733 (1985).
- ¹⁵R. C. Frank, L. E. Rehn, and P. Baldo, *J. Appl. Phys.* **57**, 845 (1985).
- ¹⁶R. C. Frank, S. P. McManus, L. E. Rehn, and P. Baldo, *J. Appl. Phys.* **59**, 2747 (1986).
- ¹⁷A. vom Felde, J. Fink, Th. Müller-Heinzerling, J. Phlüger, B. Scheerer, G. Linker, and D. Kaletta, *Phys. Rev. Lett.* **53**, 922 (1984).
- ¹⁸C. Templier, C. Jaouen, J-P. Rivière, J. Delafond, and J. Grilhé, *C. R. Acad. Sci.* **299**, 613 (1984).
- ¹⁹J. H. Evans and D. J. Mazey, *J. Phys. F* **15**, L1-L6 (1985).
- ²⁰J. H. Evans and D. J. Mazey, *J. Nucl. Mater.* **138**, 176 (1986).
- ²¹J. H. Evans and D. J. Mazey, *Scr. Metall.* **19**, 621 (1985).
- ²²G. Deconninck and A. Lefebvre, in *International Conference on Surface Modifications of Metals by Ion beams*, Kingston Canada, July 1986 (unpublished).
- ²³A. Luukkainen, J. Keinonen, and M. Erola, *Phys. Rev. B* **32**, 4814 (1985).
- ²⁴J. Völkl and G. Alefeld, in *Hydrogen in Metals I*, Topics in Applied Physics, Vol. 28, edited by J. Völkl and G. Alefeld (Springer, New York, 1978), p. 331.
- ²⁵P. Nordlander, S. Holloway, and J. K. Nørskov, *Surf. Sci.* **136**, 59 (1983).
- ²⁶H. J. Whitlow, J. Keinonen, M. Hautala, and A. Hautojärvi, *Nucl. Instrum. Methods Phys. Res. Sect. B* **5**, 505 (1984).
- ²⁷G. Frech, G. K. Wolf, H. Damjantschitsch, H. Wieser, and S. Kalbitzer, *Nucl. Instrum. Methods Phys. Res.* **218**, 500 (1983).
- ²⁸B. Maurel and G. Amsel, *Nucl. Instrum. Methods Phys. Res.* **218**, 159 (1983).
- ²⁹J. Keinonen, A. Luukkainen, A. Anttila, and M. Erola, *Nucl. Instrum. Methods Phys. Res.* **216**, 249 (1983).
- ³⁰J. Räisänen and J. Keinonen, *Appl. Phys. A* **36**, 175 (1985).
- ³¹M. Hautala, *Radiat. Eff.* **51**, 35 (1980).
- ³²L. W. Finger, R. M. Hazen, G. Zou, H. K. Mao, and P. M. Bell, *Appl. Phys. Lett.* **39**, 892 (1981).
- ³³P. Hautojärvi, H. Huomo, M. Puska, and A. Vehanen, *Phys. Rev. B* **32**, 4326 (1985).
- ³⁴A. Van Veen, W. Th. M. Buters, T. R. Armstrong, B. Nielsen, K. T. Westerduin, L. M. Caspers, and J. Th. M. de Hosson, *Nucl. Instrum. Methods Phys. Res.* **209/210**, 1055 (1983).
- ³⁵A. Van Veen, J. H. Evans, W. Th. M. Buters, and L. M. Caspers, *Radiat. Eff.* **78**, 53 (1983).
- ³⁶J. R. Beeler, *Phys. Rev. A* **134**, 1396 (1964).
- ³⁷R. H. J. Fasteman, C. M. Van Baal, P. Penning, and A. Van Veen, *Phys. Status Solidi A* **52**, 577 (1979).